Available online at www.sciencedirect.com
ScienceDirect
Trans. Nonferrous Met. Soc. China 23(2013) 3685−3690
Transactions of Nonferrous Metals Society of China
www.tnmsc.cn

Preparation and performance of hierarchically porous carbons as oxygen electrodes for lithium oxygen batteries

Yun-feng SONG, Xian-you WANG, Yan-song BAI, Hao WANG, Ben-an HU, Hong-bo SHU, Xiu-kang YANG, Lan-hua YI, Bo-wei JU, Xiao-yan ZHANG

Key Laboratory of Environmentally Friendly Chemistry and Applications of Ministry of Education, School of Chemistry, Xiangtan University, Xiangtan 411105, China

Received 27 April 2013; accepted 30 October 2013

Abstract: The hierarchically porous carbons (HPCs) were prepared by sol−gel selassembly technology in different surfactant concentrations and were used as the potential electrode for lithium oxygen batteries. The physical and electrochemical properties of the as-prepared HPCs were investigated by filed emission scanning electron microscopy (FE-SEM), transmission electron microscopy (TEM), nitrogen adsorption–desorption isotherm and galvanostatic charge/discharge. The results indicate that all of the HPCs mainly possess mesoporous structure with nearly similar pore size distribution. Using the HPCs as the electrode, a high discharge capacity for lithium oxygen battery can be achieved, and the discharge capacity increases with the specific surface area. Especially, the HPCs-3 oxygen electrode with CTAB concentration of 0.27 mol/L exhibits good capacity retention through controlling discharge depth to 800 mA·h/g and the highest discharge capacity of 2050 mA·h/g at a rate of 0.1 mA/cm^2.
Key words: lithium oxygen battery; hierarchically porous carbon; oxygen electrode; oxygen reduction

1 Introduction

Metal oxygen batteries have much higher specific energy than most available primary and rechargeable batteries in which their active cathode materials, and oxygen can be accessed from the environment. Lithium air (oxygen) batteries have the highest theoretical specific energy among all metal oxygen batteries because of the high specific energy of lithium metal. The theoretical specific energy of lithium air (oxygen) batteries is 11140 W·h/kg, excluding O_2 (5200 W·h/kg including O_2). The present lithium air (oxygen) cell appears to be rechargeable due to the use of nonaqueous electrolyte [1−3]. The first lithium oxygen battery with nonaqueous polymer electrolyte was reported in 1996 by ABRAHAM and JIANG [4]. Prototype lithium oxygen batteries typically consist of a lithium-metal anode, organic electrolyte and a porous carbon-based cathode exposed to gaseous O_2 during cell operation [5]. In an organic system, the discharge mechanism was determined to be primarily the deposition of Li_2O_2 in the porous structure of the oxygen electrode, and discharge ceases when the porous cathode is completely filled with these reaction precipitates.

There is an urgent need to design and synthesize a highly effective carbon cathode for high-performance lithium oxygen batteries. Recently, intensive research effort has been devoted to improve the performance of lithium oxygen batteries by tuning the morphology and structure of the carbon cathode. KUBOKI et al [6] compared the effect of the specific surface area and pore volume of porous carbon on discharge performance of lithium oxygen battery. It has been found that the pore volume has a more marked effect on specific capacity than the surface area. Another study carried out by YANG et al [7] showed that the porous carbon material with a significantly lower surface area but a much larger pore size displayed much better electrochemical performance than one with higher surface area but smaller pore size. And different kinds of carbon, including high-surface area carbons [8−12], mesocellular carbons, carbon nanotube [13−16], carbon fiber or carbon paper [17], and graphene [18−20], have been

Foundation item: Projects (51272221, 51072173, 21203161) supported by the National Natural Science Foundation of China; Project (10CY005) supported by Industrial Project of Colleges and Universities of Hunan Province, China
Corresponding author: Xian-you WANG; Tel: +86-731-58292060; E-mail: wxianyou@yahoo.com
DOI: 10.1016/S1003-6326(13)62917-9

used as O_2 electrodes in lithium oxygen battery. However, different kinds of porous carbon materials represent apparently different characteristics when they are used as oxygen electrode. Among all porous carbon materials, the mesoporous carbon materials lead the electrolyte ions to transport into the bulk of material quickly and also provide larger space for formation of discharge products, thus the mesoporous carbon materials are often used to improve discharge performance of the lithium oxygen batteries [21]. In contrast, the porous carbon materials with micropore size are not be suitable in lithium oxygen batteries because small pores could be easily choked by discharge product [22].

Hierarchical porous carbons (HPCs) with a multimodal pore size distribution of micro-, meso- and/or macro-pores show high electrochemically accessible surface area, short diffusion distance, and high mass transfer rate when used as electrode materials in energy storage devices [23−25]. If the size of pore is further controlled, it will reveal some excellent electrochemical performance, so it will be an interesting work for using the hierarchical porous carbons with mesoporous structure as the oxygen electrode of lithium oxygen battery. Recently, our group has carried out a lot of researches on hierarchical porous carbon materials and their supercapacitive behaviors [26−30]. In this work, the hierarchically porous carbons (HPCs) with meso-porous structure are prepared by sol–gel self-assembly process with nickel oxides and surfactant as the templates and are used as oxygen electrode of lithium oxygen batteries. The discharge behavior and battery characteristics of lithium oxygen battery are investigated in detail.

2 Experimental

Hierarchically porous carbons [26] were prepared by carbonization and corrosion of the dual template precursor. A solution of phenolic resin (PF) in ethanol as the source of carbon was added into the mixture of cetyltrimethyl ammonium bromide (CTAB), nickel nitrate hexahydrate ($Ni(NO_3)_2·6H_2O$) and sodium hydroxide (NaOH) with sufficiently stirring. The mixture was left with a blending-layered-settlement program and dried in air at 60 °C for 12 h. The sample was heated to 200 °C (5 °C/min) and maintained for 2 h in pure argon, then heated to 600 °C (5 °C/min) and maintained for 5 h, and finally cooled down naturally to room temperature. The resultant product was etched with 3 mol/L HCl thoroughly to remove $Ni(OH)_2$/NiO, then filtered and washed several times with deionized water and dried in an oven at 100 °C, finally treated with 2 mol/L HNO_3. During preparation process, the molar ratios of $Ni(NO_3)_2$ and CTAB were 4:0, 4:2, 4:4, and 4:6, and the corresponding CTAB template concentrations were 0, 0.14, 0.27, and 0.41 mol/L, respectively. The as-prepared samples were denoted as HPCs-1, HPCs-2, HPCs-3, and HPCs-4, respectively.

The porous properties of HPCs were characterized by adsorption experiments of nitrogen, and adsorption/desorption isotherms of nitrogen were measured at 77 K on a Quantachrome autosorb automated gas sorption system. The estimation of the Brunauer–Emmett–Teller (BET) specific surface area (SSA), pore volume and pore size distribution (PSD) were carried out according to the Barrett–Joyner–Halenda (BJH). Filed emission scanning electron microscope (FE-SEM) (Sirion 200, FEI) and transmission electron microscope (TEM) (JEM−2100F, JEOL) were used to study the morphology and size of HPCs.

The oxygen electrode was fabricated by compressing a mixture of carbon material (HPCs) and poly (vinylidene fluoride) binder with a mass ratio of 9:1 onto a nickel foam current collector. The geometric surface area of the oxygen electrode disks was kept to be 0.785 cm^2 and the typical loading of the oxygen electrode was 5 mg/cm^2.

The electrochemical characterizations were carried out using Swagelok type cell witch components consisting of a nickel foam as the cathode current collector and a lithium metal foil as anode. A commercial electrolyte solution of 1 mol/L $LiPF_6$ in a mixture of mass fraction of ethylene carbonate (EC)/dimethyl carbonate (DMC) 1:1 was impregnated into membrane as separator and sandwiched between a lithium metal anode and oxygen cathode.

The cells were tested in a sealed oxygen chamber under oxygen flow, and the oxygen pressure was maintained at normal pressure. The cell was cycled in Neware battery test system BTS-XWJ-6.44S-00052 (Newell, Shenzhen, China) with a voltage range of 2.0−4.5 V (vs Li^+/Li) at different current densities, which can control the test conditions such as the voltage, current, capacity and time of the charge and discharge.

3 Results and discussion

The nitrogen adsorption/desorption isotherms at 77 K for HPCs marked with HPCs-1, HPCs-2, HPCs-3, HPCs-4, respectively, are shown in Fig. l(a). As shown in Fig. 1(a), all isotherms are type IV isotherm according to the IUPAC classification [31]. High adsorption of nitrogen occurs in the low relative pressure (p/p_0) range, and obvious hysteresis is detected, suggesting the existence of micro-pores and meso-pores in HPCs [31]. A hysteresis between adsorption and desorption branches can be observed at medium relative pressure (0.4−1.0), which demonstrates the presence of a large number of

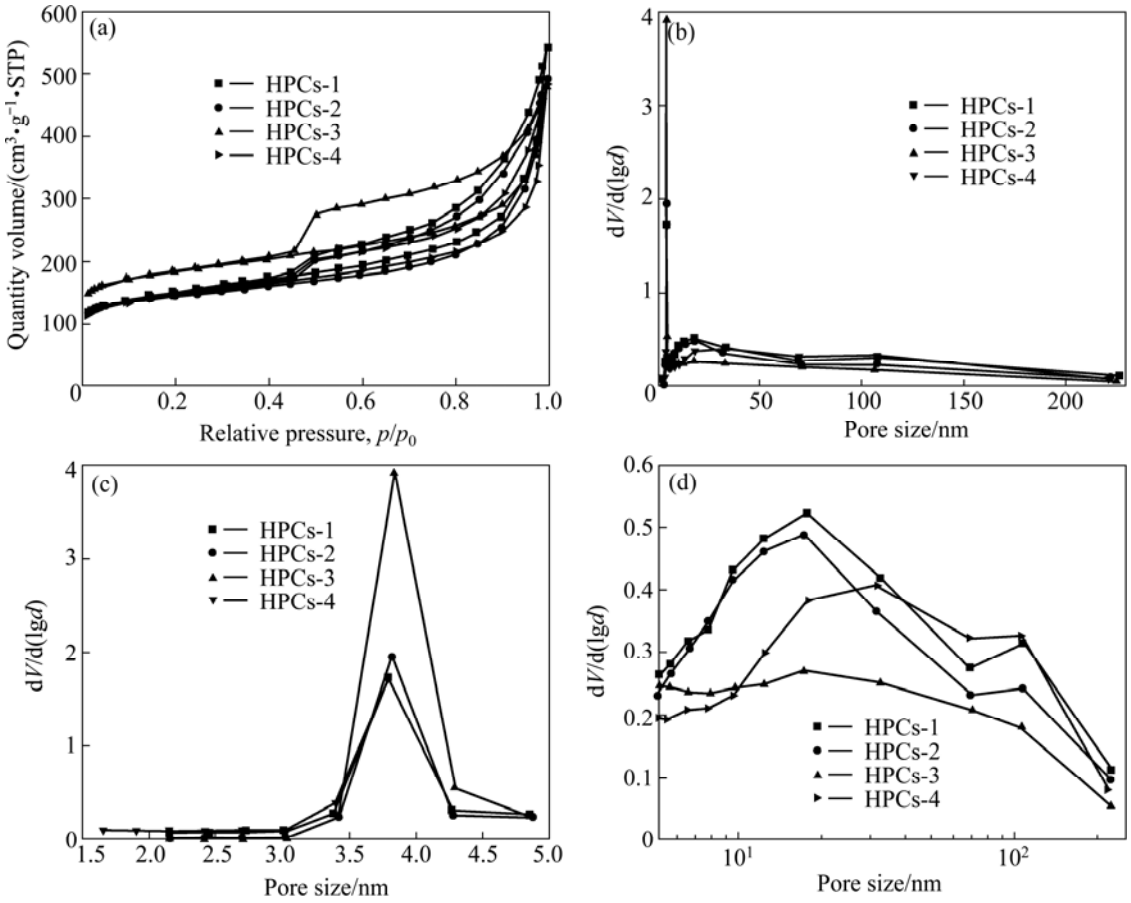

Fig. 1 Nitrogen adsorption/desorption isotherms of HPCs at 77 K (a) and whole (b) and local (c, d) pore size distribution of HPCs

mesopores. Furthermore, the isotherms rise sharply at relative pressure p/p_0 close to 1, which reveals the existence of macro-pores. Apparently, the as-prepared porous carbon materials are a combination of micro-, meso- and/or macro-pores with multimodal pore size distribution. The BET surface area, pore size and total pore volume of HPCs are summarized in Table 1. It can be known from Table 1 that the Brunauer–Emmett–Teller (BET) surface areas of HPCs are 539, 546, 691, and 535 m^2/g for HPCs-1, HPCs-2, HPCs-3, and HPCs-4, respectively; whereas the meso-pores volumes are 0.31, 0.34, 0.39, and 0.35 cm^3/g for the above corresponding materials. Besides, it can be found that the concentration of CTAB may also affect the meso-pores volume of the samples. When the concentration of CTAB is less than 0.27 mol/L, there are few meso-pores in the materials; when the concentration of CTAB is more than 0.27 mol/L, with the increase of CTAB the meso-pores volume in the materials may collapse and gradually convert into macro-pores in the carbonization process. Thus, the HPCs-3 has the largest specific surface area and meso-pore volume among all the HPCs. It may be probably attributed to the synergistic effect of dual-template when the concentration of CTAB is 0.27 mol/L [27].

Table 1 Pore structure characteristics of HPCs prepared under different conditions

Sample	c(CTAB)/ (mol·L^{-1})	S_{BET}/ ($m^2 \cdot g^{-1}$)	Pore size/ nm	V_{total}/ ($cm^3 \cdot g^{-1}$)	V_{meso}/ ($cm^3 \cdot g^{-1}$)
HPCs-1	0	539	3.80	0.76	0.31
HPCs-2	0.14	546	3.81	0.66	0.34
HPCs-3	0.27	691	3.84	0.60	0.39
HPCs-4	0.41	535	3.79	0.65	0.35

The pore volumes and pore size distribution curves of HPCs which are determined by BJH method are clearly illustrated in Fig. 1(b). The pore size distribution curves are centred in the same pore diameter range, indicating that all porous carbon samples are mainly meso-porous structure and possess similar pore size and pore size distribution. The pores size is between 3.79 and 3.84 nm. Comparatively, HPCs-3 primarily consists of meso-pores.

The surface morphology of HPCs-3 was characterized by FE-SEM and TEM, and the typical results are shown in Fig. 2. The network structure of the HPCs-3 is evidently displayed in Figs. 2(a) and (b). TEM observations were conducted to study the porous textures of the framework walls with representative areas, as

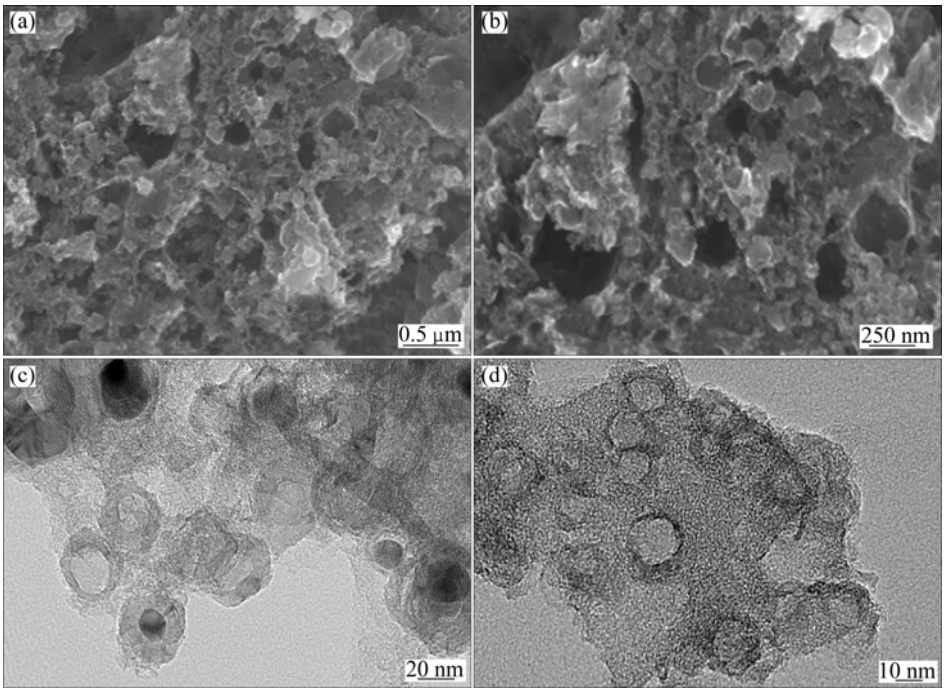

Fig. 2 FE-SEM (a, b) and TEM (c, d) images of HPCs-3

shown in Figs. 2(c) and (d). It can be observed that HPCs-3 consists of numerous macro-pores (Figs. 2(a) and (b)), which are open holes, and a lot of meso-pores distribute on the wall of macro-pores (Figs. 2(b) and (d)). When the macro-pore cores extend into the particles, they can form ion-transport path. As soon as the macro-pore cores are immersed in the electrolyte, the walls of the pore are fully covered by electrolyte, thus giving a shorter diffusion path. Also, the meso-pores can facilitate O_2 diffusion, leading the electrolyte ions to transport into the bulk of material quickly and also providing enough large volume for the discharged products.

The electrochemical performance of HPCs as oxygen electrode of lithium oxygen cell was investigated. Figure 3 shows the discharge behavior of lithium oxygen cells using various HPCs as oxygen electrodes at a constant current density 0.10 mA/cm^2 and in the voltage range of 2.0−4.5 V at room temperature. As seen from Fig. 3, all the curves show smooth and monotonous profiles. The HPCs based oxygen electrodes exhibit excellent electrochemical performance, especially the HPCs-3 owns the highest initial discharge capacity of 2050 mA·h/g. Obviously, the HPCs-3 reveals better performance due to its highest meso-pore volume and specific surface area [5]. This is likely due to the increase in storage space available for the accommodation of discharge product Li_2O_2 [21]. The discharge process is considered to cease when the pores are choked with discharge product. Therefore, the relatively low discharge capacities associated with samples of lower

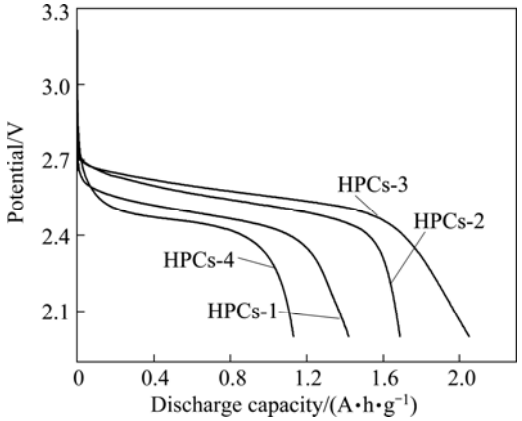

Fig. 3 Initial discharge curves of HPCs at current density of 0.10 mA/cm^2

pore volumes are due to a reduced amount of available space for storage of discharge product [32].

The initial open circuit voltages of the cell for different HPCs as oxygen electrodes vary in the range of 3.0−3.2 V (Fig. 3). These values are higher than the theoretical voltage of 2.96 V calculated by the thermodynamics of the reaction of Li and O_2 to form Li_2O_2 [33]. Higher open circuit voltage of the cell compared with the theoretical voltage may be due to a mixed potential effect associated with reaction of Li ions and impurities in the electrolyte [34].

Decrease of capacity with the increase of current density is currently another serious issue for lithium oxygen battery. In order to assess the power capabilities of the lithium oxygen cells, the electrochemical performance of the cells was analyzed at different

discharge rates. As shown in Fig. 4, the cell using HPCs-3 as oxygen electrode delivers a specific capacity of 2667 mA·h/g at a low current density of 0.05 mA/cm^2. However, the specific capacity and operating voltage drop significantly with the increase of current density. The discharge capacities of HPCs-3 oxygen electrode at different discharge current densities are 2667, 2050, 1206, 607 mA·h/g, at discharge currant density of 0.05, 0.10, 0.20 and 0.50 mA/cm^2 respectively. The HPCs-3 exhibits a relatively poor rate capability. The inherent limitation of lithium oxygen battery, the limited oxygen solubility and diffusivity significantly affect the rate capability of the cell since there is no enough oxygen to enable the discharge reaction at a high current density [28].

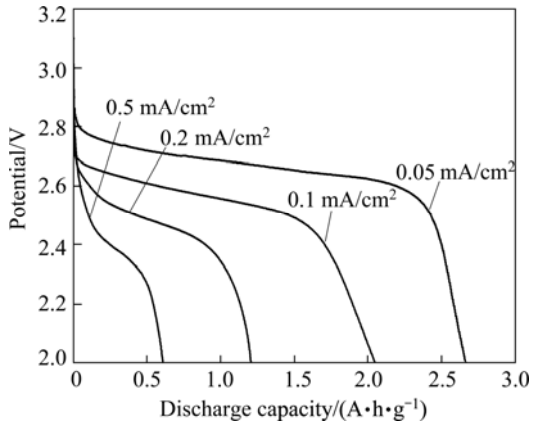

Fig. 4 Discharge curves of HPCs-3 at different discharge rates

The cycle performance of the lithium oxygen cell using HPCs-3 as oxygen electrode is shown in Fig. 5. In the case of deep discharge with a cut-off voltage of 2.0 V, a relatively high initial discharge capacity of about 2050 mA·h/g was obtained (Fig. 5(a)); however, the capacity retention remains rather poor with the discharge capacity dramatically dropping to 670 mA·h/g after 10 cycles. The poor capacity retention of the cell could be attributed to the continuous rise of resistance which results from the aggregation of discharge product. By avoiding deep discharge and restricting discharge capacity only to 800 mA·h/g, the cell exhibits a good capacity retention after 10 cycles. As shown in Fig. 5(b), it is nearly a horizontal line after the 10th cycle. It may be ascribed to the problem settled that pores can be easily choked by discharge product [35]. In this condition, even if the electrode expands, the electrical contact between the active materials and current collector is still good. Moreover, Li_2O_2 and Li_2O decomposition during the charge process renews the porosity and makes further cycle possible.

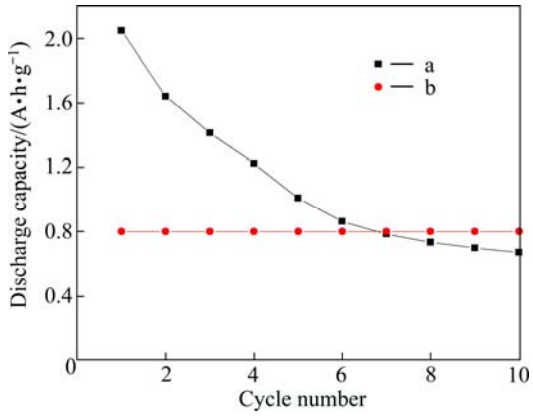

Fig. 5 Cycle performance of lithium oxygen cells in condition of deep discharge (a) and only restricting charge/discharge capacity to 800 mA·h/g (b)

4 Conclusions

1) Various HPCs with meso-porous structure were successfully synthesized by self-assembly process via adjusting surfactant concentration.

2) All of the synthesized HPCs mainly possess meso-porous structure with similar pore size distribution. Especially, the HPCs-3 prepared at *c*(CTAB)=0.27 mol/L shows the largest mespores volume of 0.35 cm^3/g, and the highest discharge capacity of 2050 mA·h/g at the current density of 0.10 mA/cm^2.

3) The discharge capacity of the lithium oxygen battery using HPCs as air electrode will be improved with the increasing specific surface area at nearly same pore size. Besides, the lithium air battery exhibits a good capacity retention through controlling discharge depth to 800 mA·h/g.

4) Although the rate capability of HPCs-3 air electrode needs to be further improved, it will be a kind of promising air electrode for the application of lithium oxygen batteries.

References

[1] PENG Z, FREUMBERGER S A, CHEN Y. A reversible and higher-rate Li−O_2 battery [J]. Science, 2012, 337(6094): 563−566.

[2] CAI K, PU W, GAO Y. Investigation of ionic liquid composite electrolyte for lithium–oxygen battery [J]. International Journal of Hydrogen Energy, 2013, 38(25): 1−5.

[3] LI L, ZHAO X, MANTHIRAM A. A dual-electrolyte rechargeable Li-air battery with phosphate buffer catholyte [J]. Electrochemistry Communications, 2012, 14(1): 78−81.

[4] ABRAHAM K M, JIANG Z. A polymer electrolyte-based rechargeable lithium/oxygen battery [J]. Journal of the Electrochemical Society, 1996, 143(1): 1−5.

[5] WANG Z L, XU D, XU J J. Graphene oxide gel-derived, free-standing, hierarchically porous carbon for high-capacity and high-rate rechargeable Li−O_2 batteries [J]. Advanced Functional Materials, 2012, 22(17): 3699−3705.

[6] KUBOKI T, OKUYAMA T, OHSAKI T, TAKAMI N. Lithium-air batteries using hydrophobic room temperature ionic liquid electrolyte [J]. Journal of Power Sources, 2005, 146(1): 766−769.

[7] YANG X, HE P, XIA Y. Preparation of mesocellular carbon foam and its application for lithium/oxygen battery [J]. Electrochemistry Communications, 2009, 11(6): 1127−1130.

[8] KWON S H, JEONG Y K, KWON S, KANG M C, LEE H W.

Dielectrophoretic assembly of semiconducting single-walled carbon nanotube transistor [J]. Transactions of Nonferrous Metals Society of China, 2011, 21: s126−s129.
[9] XIAO J, WANG D, XU W. Optimization of oxygen electrode for Li/air batteries [J]. Journal of the Electrochemical Society A, 2010, 157(4): 487−492.
[10] ZHANG W. Calculation model of edge carbon atoms in graphite particles for anode of lithium-ion batteries [J]. Transactions of Nonferrous Metals Society of China, 2011, 21(11): 2466−2475.
[11] BEATTIE S D, MANOLESCU D M, BLOXYGEN S L. High-capacity lithium–air cathodes [J]. Journal of the Electrochemical Society A, 2009, 156(1): A44−A47.
[12] PARK C K, PARK S B, LEE S Y. Electrochemical performances of lithium-air cell with carbon materials [J]. Bull Kor Chem Soc, 2010, 31: 3221−3224.
[13] YOO E, NAKAMURA J, ZHOU H. N-doped graphene nanosheets for Li–air fuel cells under acidic conditions [J]. Energy & Environmental Science, 2012, 5(5): 6928−6932.
[14] YAN X B, GU Y H, HUANG D, GAN L, W L X, HUANG L H, CHEN Z D, HUANG S P, ZHOU K C. Binding tendency with oligonucleotides and cell toxicity of cetyltrimethyl ammonium bromide-coated single-walled carbon nanotubes [J]. Transactions of Nonferrous Metals Society of China, 2011, 21(5): 1085−1091.
[15] LIM Y J, PARK M Y, LEE S K, LEE W K, JO N J. Polyaniline and multi-walled carbon nanotube composite electrode for rechargeable battery [J]. Transactions of Nonferrous Metals Society of China, 2012, 22: s717−s721.
[16] KWON S, KIM S H, KIM K, KIM K H, KANG M C, LEE H W. Distribution of electric field for carbon nanotube assembly: Experiments (II) [J]. Transactions of Nonferrous Metals Society of China, 2011, 21: s121−s125.
[17] ZHANG G Q, ZHENG J P, LIANG R. Lithium–air batteries using SWNT/CNF buckypapers as air electrodes [J]. Journal of the Electrochemical Society A, 2010, 157(8): 953−956.
[18] LI Y, WANG J, LI X. Superior energy capacity of graphene nanosheets for a nonaqueous lithium-air battery [J]. Chemical Communications, 2011, 47(33): 9438−9440.
[19] SUN B, WANG B, SU D. Graphene nanosheets as cathode catalysts for lithium-air batteries with an enhanced electrochemical performance [J]. Carbon, 2012, 50(2): 727−733.
[20] REN X, ZHANG S S, TRAND T. Oxygen reduction reaction catalyst on lithium/air battery discharge performance [J]. Journal of Materials Chemistry, 2011, 21(27): 10118−10125.
[21] MIRZAEIAN M, HALL P J. Preparation of controlled porosity carbon aerogels for energy storage in rechargeable lithium oxygen batteries [J]. Electrochimica Acta, 2009, 54(28): 7444−7451.
[22] ZHANG S S, FOSTER D, READ J. Discharge characteristic of a non-aqueous electrolyte Li/O_2 battery [J]. Journal of Power Sources, 2010, 195(4): 1235−1240.
[23] ZUO S, XIAO Y, LIU Y. Green and low-cost materials as carbon source for the synthesis of hierarchical porous carbons [J]. Journal of Materials Science, 2010, 45(16): 4439−4443.
[24] CHENG Q, XIA Y, PAVLINEK V. Effects of macropore size on structural and electrochemical properties of hierarchical porous carbons [J]. Journal of Materials Science, 2012, 47(17): 6444−6450.
[25] LIU Y, LI K, WANG J, SUN G, SUN C. Preparation of spherical activated carbon with hierarchical porous texture [J]. Journal of Materials Science, 2009, 44(17): 4750−4753.
[26] LI Na, WANG Xian-you, WEI Jian-liang, AN Hong-fang, ZHENG Li-ping. Template synthesis of mesoporous carbon and its application in supercapacitors [J]. The Chinese Journal of Nonferrous Metals, 2009, 40(3): 601−607. (in Chinese)
[27] LI Jiao-jiao, WANG Xian-you, YANG Shun-yi, LONG Wan-mei. Preparation and electrochemical performance of calcium carbide skeleton carbon anode material for lithium ion battery [J]. The Chinese Journal of Nonferrous Metals, 2011, 21(12): 3087−3093. (in Chinese)
[28] ZHANG X, WANG X, BAI Y. Supercapacitive behaviors of hierarchically porous carbons prepared by metal oxide/surfactant templates [J]. Journal of the Electrochemical Society A, 2012, 159(4): 431−437.
[29] ZHANG X, WANG X, SU J, WANG X, JIANG L, WU H, WU C. The effects of surfactant template concentration on the supercapacitive behaviors of hierarchically porous carbons [J]. Journal of Power Sources, 2012, 199: 402−408.
[30] SING K S W, EVERETT D H, HAUL R A W, PIEROTT L, ROUQUERO R, SIEMIENIEWASA J T. Physical and biophysical chemistry division commission on colloid and surface chemistry including catalysis [J]. Pure and Applied Chemistry, 1985, 57(4): 603−619.
[31] THOMMES M. Physical adsorption characterization of nanoporous materials [J]. Chemie Ingenieur Technik, 2010, 82(7): 1059−1073.
[32] SHITTA-BEY G O, MIRZAEIAN M, HALL P J. The electrochemical performance of phenol-formaldehyde based activated carbon electrodes for lithium/oxygen batteries [J]. Journal of the Electrochemical Society A, 2012, 159(3): 315−320.
[33] YOUNESI R, HAHLIN M, EDSTROM K. Surface characterization of the carbon cathode and the lithium anode of Li−O_2 batteries using $LiClO_4$ or LiBOB salts [J]. ACS Applied Materials & Interfaces, 2013, 5: 1333−1341.
[34] GIRISHKUMAR G, MCCLOSKEY B, LUNTZ A C. Lithium−air battery: Promise and challenges [J]. The Journal of Physical Chemistry Letters, 2010, 1(14): 2193−2203.
[35] ZHANG D, LI R, HUANG T. Novel composite polymer electrolyte for lithium air batteries [J]. Journal of Power Sources, 2010, 195(4): 1202−1206.

锂空气电池空气电极层次多孔碳的制备及其性能

宋云峰，王先友，白艳松，王 灏，胡本安，舒洪波，杨秀康，易兰花，鞠博伟，张小艳

湘潭大学 化学学院，环境友好化学与应用教育部重点实验室，湘潭 411105

摘 要：在不同表面活性剂浓度下通过溶胶−凝胶自组装方法制备了具有介孔结构的层次多孔碳材料(HPCs)。用场发射扫描电镜(FE-SEM)、透射电镜(TEM)、氮气吸脱附测试和恒流充放电测试对样品进行物理和电化学性能研究。结果表明：所有的 HPCs 主要为介孔结构并且具有相似的孔径分布。以 HPCs 为空气电极载体碳材料的锂空气电池具有较高的放电容量。且相似孔径大小的碳材料为载体的锂空气电池放电容量随着碳材料的比表面积增加而增加。在 *c*(CTAB)=0.27 mol/L 时制备的 HPCs-3 样品具有最佳的电化学性能。通过控制放电深度至 800 mA·h/g，电池表现出良好的容量保持率，在 0.1 mA/cm^2 电流密度下，首次放电容量为 2050 mA·h/g。

关键词：锂氧电池；层次多孔碳；氧电极；氧还原

(Edited by Hua YANG)